High-Temperature Heterogeneous Catalysis in Platinum Nanoparticle – Molten Salt Suspensions

SCHOLARONE™
Manuscripts

COMMUNICATION

High-Temperature Heterogeneous Catalysis in Platinum Nanoparticle – Molten Salt Suspensions

Behzad Tangeysh[a], Clarke Palmer[a], Horia Metiu[b], Michael J. Gordon[a], and Eric W. McFarland*

Suspensions of platinum nanoparticles (PtNP) were formed in molten LiCl-LiBr-KBr via thermal decomposition of H_2PtCl_6, and subsequently evaluated for thermal stability and CO oxidation activity. Significant nanoparticle (NP) aggregation was observed above 500 °C, and the heat capacity of the melt with PtNPs was 47% higher than the salt alone, further increasing with NP concentration. CO oxidation was observed when PtNPs were present in the melt, which, together with measured changes in surface tension, support the hypothesis that gas-solid catalysis at the gas-nanoparticle-melt interface is indeed possible, opening up a new approach for heterogeneous catalysis.

Synthesis and use of metal nanoparticles (MNPs) has been widely studied in many fields ranging from catalysis to medicine.[1-3] MNPs are commonly formed in aqueous solutions and organic solvents in the presence of surfactant molecules and/or polymer capping agents.[4-6] The use of surfactants provides colloidal stability, prevents rapid aggregation, and directs the size and morphology of the NPs.[7, 8]

Ionic liquids have also been considered as an alternative solvent medium for producing MNPs.[9, 10] Ionic liquids are low-temperature electrolytes with organic constituents acting as a template for the synthesis and stabilization of MNPs.[11] Nanoscale metal particles formed in ionic liquids have been extensively used for catalyzing a variety of organic transformations including olefin hydrogenation and C–C cross coupling reactions.[12, 13] The use of ionic liquids as an environment for catalysis is mainly due to their negligible vapor pressure, high ionic conductivity, and favorable heat transfer properties as compared to other common solvents.[10,14] However, the poor thermal stability of the ionic liquids' organic counterpart significantly restricts the use of these nanofluids for high temperature reactions.[15, 16]

Traditional molten salt electrolytes with inorganic constituents, i.e. alkali metal halides, have excellent thermal stability and can be used as a solvent for multi-phase high-temperature catalytic reactions.[17,18] These strong electrolyte melts have been recently considered as a new medium for producing a variety of nano/micro- scale materials including metal and metal oxides, as well as carbon nanostructures.[19] Various methods have been developed to produce MNPs in a melt, and the applications of these complex fluids as thermal energy storage and heat transfer fluids have been extensively investigated.[20-23] Heat capacity increases ranging from ~5% to 100% have been reported for these high-temperature complex mixtures,[24-27] yet no comprehensive explanation has been presented for these experimental observations.

Most recently, Srivastava *et al.* showed the synthesis of luminescent quantum dots by manipulating the composition of the semiconductor NPs in the melt, where the required reaction temperature is not accessible by traditional colloidal synthesis techniques.[28] Zhang *et al.* also showed that the phase-transfer of pre-formed NPs can be used to form MNP suspensions in the melt, where the interactions between the salt constituents and the surface of NPs determine the stability of colloidal particles.[29] The importance of the salt-metal interaction in catalysis was investigated in work by Kusche et al[30] where the reforming of methanol with steam on commercial supported Pt catalysts was shown to be strongly promoted by contact with a molten alkali salt.

Herein, we present results on the formation, stability, and reactivity of PtNPs suspended in molten alkali metal halides to gas-phase molecules. PtNPs have been extensively used in heterogeneous catalysis of gaseous reactants, including CO oxidation and alkane activation.[31-33] For suspensions of PtNPs in molten alkali halide salts, we examined the following questions: (1) Can MNPs be produced in molten halide host salts?, (2) What is the thermal stability and heat capacity of the nanofluid suspension?, and (3) Are the MNPs suspended in the salt active as heterogeneous catalysts for gaseous reactants?

A ternary mixture of LiCl-LiBr-KBr (%mole= 25:37:38) with a melting point of ~330°C was used as a solvent for the NP synthesis (details in SI†). This mixture was previously used to stabilize pre-formed NPs in molten salts.[29] Heating of the host salt in a tubular high-temperature furnace resulted in a colorless liquid at 350°C (Fig. 1(a)). Addition of 60μL H_2PtCl_6 (0.05M) to the salt (0.015 wt% of Pt salt) before heating leads to the appearance of a homogeneous grey liquid after complete melting of the mixture (Fig. 1(b)). This suggests the formation of colloidal PtNPs suspended in molten LiCl-LiBr-KBr. We also observed purple and grey liquids after melting the salt with

[a.] Department of Chemical Engineering, University of California, Santa Barbara, CA 93106-5080

[b.] Department of Chemistry and Biochemistry, University of California, Santa Barbara, CA 93106-9510Address here.

0.015 wt% K_2PdCl_4 and $HAuCl_4$, respectively, which implies that Pd and Au NPs were formed during heating of the metal chloride anions (i.e., $[MCl_x]^y$) in LiCl-LiBr-KBr (Fig. S1†).

PtNPs in the (solidified) melt were observed by electron microscopy (Fig. 1(c-e)) after cooling the liquids. In the low-magnification SEM images, large salt features (Fig. 1(c)) were observed, and confirmed by energy dispersive X-ray spectroscopy (EDS) (Fig. S2†). In high-magnification SEM images, bright features embedded in the salt were observed (Fig. 1(d)). Elemental mapping and back-scattering measurements performed on the sample confirmed that the observed high-contrast features were PtNPs (Fig. 1(d) and S2†). Transmission electron microscopy (TEM) was used to measure the size of PtNPs (Fig. 1(e) and S3†). After removal of the host salt, spherical and semi-spherical PtNPs were observed with sizes ranging from 5-25nm (Fig. 1(e)). These observations support that during heating, simultaneous melting of LiCl-LiBr-KBr and H_2PtCl_6 leads to the formation of PtNPs in the absence of a reducing agent by thermal decomposition[34] of the Pt complex (eq.1), followed by agglomeration of Pt^0 species (eq.2) as the dominant pathway for PtNP formation:

$$(1) H_2PtCl_6 \rightarrow PtCl_4 + 2HCl \rightarrow PtCl_2 + Cl_2 \rightarrow Pt^0 + Cl_2$$
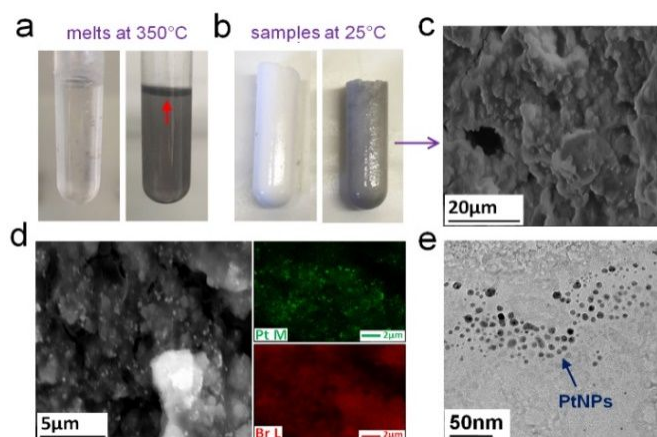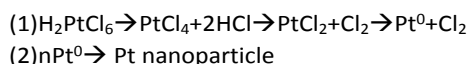$$(2) nPt^0 \rightarrow \text{Pt nanoparticle}$$

Fig. 1 (a,b) Photographs of LiCl-LiBr-KBr with (grey) and without (clear) PtNPs at 350°C (a) and room temperature (b). The black layer on top of grey melt corresponds to the meniscus of Pt nanofluid (red arrow). (c) Low-magnification SEM of Pt nanofluid recorded after complete cooling of the mixture. (d) High-magnification SEM and elemental mapping of Pt nanofluid (gray sample) shown in panels (a,b). (e) TEM image of PtNPs produced in the melt recorded after complete removal of the host salt by DI water washing.

An apparatus shown schematically in Fig. 2(a) was used to measure the UV-visible spectra of nanofluids (details in SI†). As shown in Fig. 2(b) (purple curve), a broad absorption feature related to the NPs light scattering was observed in the spectra of Pt nanofluid. This is similar to the spectra of PtNPs suspended in aqueous and organic solvents.[35,36] The corresponding absorption characteristics of Pd and AuNPs[37,38] were also observed in the spectra of nanofluids formed upon melting the salt in the presence of K_2PdCl_4 and $HAuCl_4$ (Fig. S4†). These observations in molten alkali halide salts are similar to those in other common solvent environments. The spectrum of molten LiCl-LiBr-KBr (red curve) recorded at 350°C shows only a weak

absorption at ~330 nm. This band corresponds to the charge transfer of anions to the surrounding cations in alkali metal halides as reported previously.[39]

The spectra of suspensions were measured as a function of temperature to determine the stability of Pt nanofluids. Increasing the temperature of the fluid from 400°C to 650°C resulted in a decrease in the absorption of Pt fluid sample (Fig. S5†). As shown in Fig. 2(c), a rapid decrease was observed in the absorption of NPs recorded at 500nm between 475°C and 575°C. This suggests that the PtNPs quickly agglomerate above 500°C, and is consistent with the photographs recorded in the screening experiments as a function of temperature (inset of Fig. 2(c)). The absorbance of NPs as a function of time between 350°C and 400°C shows no significant change (Fig. S6†). To investigate colloidal stability at temperatures below the aggregation limit, time-dependent UV-vis were performed at 400°C. As shown in Fig. 2(d), the spectra of the nanofluid recorded for 350 minutes did not show significant changes in absorbance. As such, the NP suspension appears relatively stable below 500°C. Increasing the temperature from 400°C to 650°C for this sample resulted in a rapid decrease in the measured absorbance values (arrows in Fig. 2(d)).
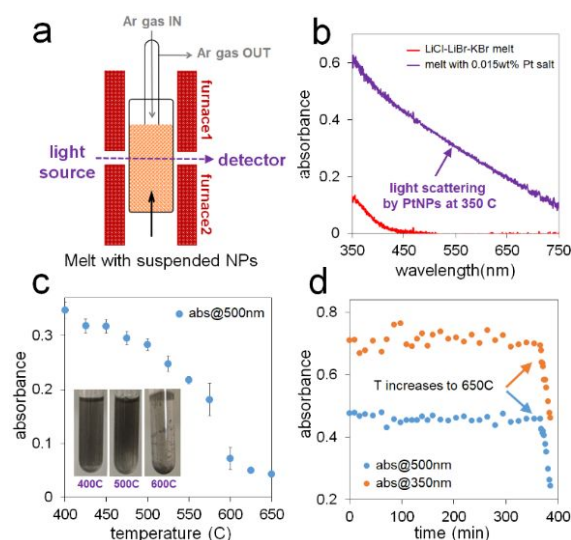

Fig. 2 (a) Scheme of UV-Visible setup used to evaluate the formation and stability of PtNPs in the melt. (b) The spectra of LiCl-LiBr-KBr (red curve), and the salt with 0.015 wt% of H_2PtCl_6 (purple curve) recorded after complete melting of the samples at 350°C. (c) temperature-dependent changes in the absorbance of PtNPs at 500 nm. The inset shows photographs of Pt nanofluid recorded at 400°C, 500°C, and 600°C. (d) Changes in the absorbance of Pt nanofluid at 350nm and 500nm vs time at 400°C. The arrows show the time when the temperature was rapidly increased to 650°C.

Differential scanning calorimetry (DSC) was performed to determine the thermal capacity of Pt nanofluids (details in SI†). For neat LiCl-LiBr-KBr, a heat capacity (Cp) of ~0.75 J/g°C was calculated at 500°C (NIST database, see SI†), which remained unchanged as a function of temperature (dotted black line in Fig. 3(a)). This is consistent with the minimal variation previously observed in the base-fluid's heat capacity vs. temperature.[26,27] In contrast, a near linear increase was observed in the C_p of Pt nanofluid vs temperature (red and

purple curves in Fig. 3(a)). For the nanofluid with 0.015 wt% Pt salt, a Cp value of 1.12 J/g °C was measured at 500°C (47% more than host salt), which further increases by ~58% to 1.72 J/g°C when the Pt salt concentration was increased by a factor of 10. Thus, the presence of suspended PtNPs in LiCl-LiBr-KBr significantly changes the melt's thermal properties, and is consistent with other reports on the enhancement of a molten salt's specific heat in the presence of MNPs.[24-26]

Measurements of surface tension (ζ) were also performed in molten LiCl-LiBr-KBr with and without PtNPs using the maximum bubble pressure method[40, 41] (details in SI†). For the host salt, ζ = 99.3 mN/m was obtained at 350°C, which near-linearly decreases to 87.9 mN/m when the temperature was increased to 625°C (Fig. 3(b), blue dots). In the Pt nanofluid (0.015 wt% Pt salt), a significantly higher surface tension (108.2 mN/m) was observed at 350°C (Fig. 3(b), red dots), which further increases to 113.8 mN/m upon increasing the wt% of Pt salt to 0.030 (in Fig. 3(b), purple dots). Increasing the temperature in both Pt fluid samples resulted in a ζ decrease, similar to that observed for the host salt. This is consistent with the changes of ζ in alkali halide melts reported previously,[42, 43] and is due to decreasing the intermolecular cohesive forces between the liquid molecules at high temperatures leading to a decreases in the melt's surface tension.

As shown in Fig. 3(b), the presence of PtNPs in the melt significantly increased the ζ values (~10-15%) recorded in the regions where PtNPs form a stable suspension. This is due to increasing the surface free energy at the liquid-gas interface, as a result of van der Waals interactions between NPs,[43,44] and suggests that the particles in the melt are localized at the gas-liquid interface of the bubble and available to interact with gas phase reagents. Decrease in the differences between the three measurements (with and without PtNPs) at temperatures above 500°C is likely due to NP aggregation, as shown by UV-Vis measurements (Fig. 2), which significantly decreases particles concentration at the gas-liquid interface.
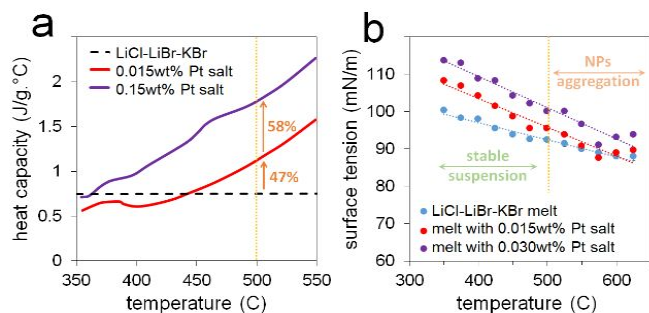
contact between the gas and metal surface. Details of activity measurements are presented in SI†. As shown in Fig. S7†, the presence of PtNPs (0.015 wt% Pt) in molten LiCl-LiBr-KBr decreased the temperature where propane dehydrogenation was observable (light off temperature) by ~100 °C. Increasing the PtNP concentration from 0.015 wt% to 0.15 wt% Pt was seen to approximately linearly increase conversion from ~0.5% to 3.5% at 400°C (Fig. S7†). These results show that the PtNPs are catalytically active in the melt and contacting the gas phase. Aggregation of NPs at temperatures >400°C resulted in a decrease in conversion (Fig. S6†), due to an effective overall decrease in surface area available for reaction. As propane dehydrogenation in the presence of Pt catalysts usually occurs at temperatures >500°C ($\Delta G°_{rxn}$= +50KJ/mole at 400°C),[45,46] the instability of Pt nanofluids at these temperatures significantly restricts achieving higher conversions.

In other experiments, we evaluated the activity of Pt nanofluids for CO oxidation (Fig. 4(b)). CO oxidation is thermodynamically favorable ($\Delta G°_{rxn}$= -220KJ/mole at 400°C) in the region where the NPs form a stable suspension (Fig. S8†), and it is well-known that reactions between CO and O_2 are catalytic on Pt surfaces.[32, 33] Our measurements, Fig. 4(b), show high reactivity (~80% conversion at 375°C) in the Pt nanofluid sample (0.15 wt% Pt) as compared to the host salt without the Pt partices.

Increasing the temperature to the point where agglomeration occurs was seen to significantly reduce the amount of CO_2 produced (Fig. 4(b), yellow arrow), similar to that observed for propane dehydrogenation. These results underscore the importance of maintaining a stable suspension to preserve the melt activity. In high temperature molten salts the stability[29] and activity of the dispersed particles will be critically dependent on the choice of the melt constituents interacting with the surface of MNPs. Varying the molten salt composition can also affect other characteristics of the nanofluids, ranging from NPs morphology to their activity as catalysts. It is well-known that the presence of halide anions , i.e. Br⁻, directs the shape of NPs in solution-phase colloidal synthesis.[7,47] Also, it has been previously reported that the presence of potassium ions enhances the catalytic activity of Pt/alumina catalysts coated with molten salts, significantly more than other alkali ions.[30] Accordingly, an important extension the work described in this Communication is an exploration of the influence of the melt composition on the nanofluid characteristics and reactivity.
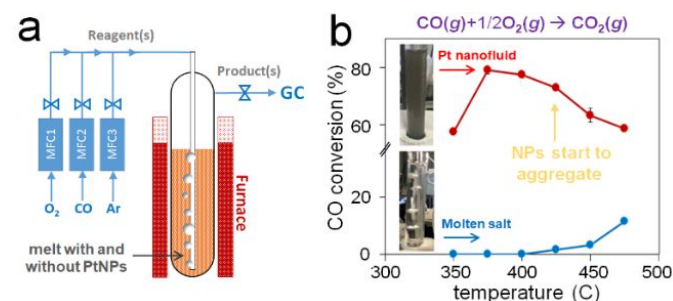

Fig. 3 (a) Normalized Cp of LiCl-LiBr-KBr with 0.015 wt% (red) and 0.15 wt% (purple) Pt salt as a function of temperature from 350°C to 550°C. The black dotted line shows the Cp of LiCl-LiBr-KBr calculated based on the NIST database (see SI†). (b) Temperature-dependent changes in surface tension for molten LiCl-LiBr-KBr (blue dots), and PtNP-salt suspensions with 0.015 wt% (red dots) and 0.030 wt% Pt (purple dots). Measurements were performed at identical conditions for all samples with 2sccm Ar flow.

Propane dehydrogenation in a bubble column reactor (Fig. 4(a)) was used as a model reaction to evaluate the activity of Pt nanofluids in heterogeneous alkane activation, which requires

Fig. 4 (a) Scheme of the bubble column reactor used to evaluate the catalytic activity of Pt nanofluids for gas-solid reactions. (b) CO conversion as a function of temperature in molten LiCl-LiBr-KBr, and in the salt with suspended PtNPs (0.15 wt% Pt). Photographs in panel (b) were recorded at 400°C during bubble column measurements. All

measurements were made at reactant flow rates of 3 sccm with a CO:O_2 mole ratio of 2:1. Error bars shown panel (b) were obtained from multiple measurements of CO by gas chromatography.

Conclusions

Pt nanoparticles can be synthesized and suspended in a salt melt (LiCl-LiBr-KBr) via thermal decomposition of metal chloride complexes. The Pt nanofluid showed good stability at temperatures below 450°C, which is ~100°C above the melting point of the host salt. This stability is most likely due to the strong interactions between bromide ions and the surface of PtNPs,[48, 49] which leads to the formation of ionic layers around the NPs, preventing rapid agglomeration via electrostatic repulsion. The observed activity for catalysis of the gas phase reactants and the significant increases in surface tension in the suspensions prove that the MNP's are present at the gas-liquid interface. The presence of PtNPs in the melt significantly enhanced the heat capacity of the melt, indicating the potential of nanofluid suspensions for heat transfer and thermal energy storage applications.

Conflicts of interest

There are no conflicts to declare.

Acknowledgements

Notes and references

1   P. K. Jain, X. Huang, I. H. El-Sayed and M. A. El-Sayed, *Acc. Chem. Res.*, 2008, **41**, 1578-1586.
2   K. An, S. Alayoglu, T. Ewers and G. A. Somorjai, *J. Colloid Interface Sci.*, 2012, **373**, 1-13.
3   A. Chen and P. Holt-Hindle, *Chem. Rev.*, 2010, **110**, 3767-3804.
4   R. Hao, R. Xing, Z. Xu, Y. Hou, S. Gao and S. Sun, *Adv. Mater. (Weinheim, Ger.)*, 2010, **22**, 2729-2742.
5   S. Guo and E. Wang, *Nano Today*, 2011, **6**, 240-264.
6   B. L. Cushing, V. L. Kolesnichenko and C. J. O'Connor, *Chem. Rev.*, 2004, **104**, 3893-3946.
7   Y. Xia, Y. Xiong, B. Lim and S. E. Skrabalak, *Angew. Chem., Int. Ed.*, 2009, **48**, 60-103.
8   B. A. Rozenberg and R. Tenne, *Prog. Polym. Sci.*, 2008, **33**, 40-112.
9   M. Antonietti, D. Kuang, B. Smarsly and Y. Zhou, *Angew. Chem., Int. Ed.*, 2004, **43**, 4988-4992.
10   Z. Ma, J. Yu and S. Dai, *Adv. Mater.* 2010, **22**, 261-285.
11   J. Dupont and J. D. Scholten, *Chem. Soc. Rev.*, 2010, **39**, 1780-1804.
12   P. Wasserscheid and W. Keim, *Angew. Chem., Int. Ed.*, 2000, **39**, 3772-3789.
13   J. D. Scholten, B. C. Leal and J. Dupont, *ACS Catalysis*, 2012, **2**, 184-200.
14   T. Welton, *Coord. Chem. Rev.*, 2004, **248**, 2459-2477.
15   Y. Cao and T. Mu, *Ind. Eng. Chem. Res.*, 2014, **53**, 8651-8664.
16   C. Maton, N. De Vos and C. V. Stevens, *Chem. Soc. Rev.*, 2013, **42**, 5963-5977.
17   W. Sundermeyer, *Angew. Chem., Int. Ed.*, 1965, **4**, 222-238.
18   C. N. Kenney, *Catalysis Reviews*, 1975, **11**, 197-224.
19   X. Liu, N. Fechler and M. Antonietti, *Chem. Soc. Rev.*, 2013, **42**, 8237-8265.
20   B. Dudda and D. Shin, *Int. J. Therm. Sci.*, 2013, **69**, 37-42.
21   X. Chen, Y.-t. Wu, L.-d. Zhang, X. Wang and C.-f. Ma, *Sol. Energy Mater. Sol. Cells*, 2018, **176**, 42-48.
22   D. Shin, H. Tiznobaik and D. Banerjee, *Appl. Phys. Lett.*, 2014, **104**, 121914.
23   M. Chieruzzi, G. F. Cerritelli, A. Miliozzi and J. M. Kenny, *Nanoscale Res. Lett.*, 2013, **8**, 448.
24   D. Shin and D. Banerjee, *J. Heat Transfer*, 2013, **135**, 032801.
25   R. Hentschke, *Nanoscale Res. Lett.*, 2016, **11**, 88.
26   M. Lasfargues, A. Bell and Y. Ding, *J Nanopart Res*, 2016, **18**, 150.
27   P. Andreu-Cabedo, R. Mondragon, L. Hernandez, R. Martinez-Cuenca, L. Cabedo and J. E. Julia, *Nanoscale Res. Lett.*, 2014, **9**, 582.
28   V. Srivastava, V. Kamysbayev, L. Hong, E. Dunietz, R. F. Klie and D. V. Talapin, *J. Am. Chem. Soc.*, 2018, **140**, 12144-12151.
29   H. Zhang, K. Dasbiswas, N. B. Ludwig, G. Han, B. Lee, S. Vaikuntanathan and D. V. Talapin, *Nature*, 2017, **542**, 328.
30   M. Kusche, F. Enzenberger, S. Bajus, H. Niedermeyer, A. Bçsmann, A. Kaftan, M. Laurin, J. Libuda, and P. Wasserscheid *Angew. Chem. Int. Ed.* 2013, **52**, 5028 –5032
31   S. Vajda, M. J. Pellin, J. P. Greeley, C. L. Marshall, L. A. Curtiss, G. A. Ballentine, J. W. Elam, S. Catillon-Mucherie, P. C. Redfern, F. Mehmood and P. Zapol, *Nat. Mater.*, 2009, **8**, 213.
32   K. Ding, A. Gulec, A. M. Johnson, N. M. Schweitzer, G. D. Stucky, L. D. Marks and P. C. Stair, *Science*, 2015, **350**, 189-192.
33   A. D. Allian, K. Takanabe, K. L. Fujdala, X. Hao, T. J. Truex, J. Cai, C. Buda, M. Neurock and E. Iglesia, *J. Am. Chem. Soc.*, 2011, **133**, 4498-4517.
34   B. Xue, P. Chen, Q. Hong, J. Lin and K. L. Tan, *J. Mater. Chem.*, 2001, **11**, 2378-2381.
35   T. Herricks, J. Chen and Y. Xia, *Nano Lett.*, 2004, **4**, 2367-2371.
36   R. M. Crooks and M. Zhao, *Adv. Mater. (Weinheim, Ger.)*, 1999, **11**, 217-220.
37   B. Tangeysh, M. Fryd, M. A. Ilies and B. B. Wayland, *Chem. Commun.*, 2012, **48**, 8955-8957.
38   B. Tangeysh, K. Moore Tibbetts, J. H. Odhner, B. B. Wayland and R. J. Levis, *J. Phys. Chem. C*, 2013, **117**, 18719-18727.
39   J. Greenberg and B. R. Sundheim, *The Journal of Chemical Physics*, 1958, **29**, 1029-1032.
40   Y. Saito, H. Yoshida, T. Yokoyama and Y. Ogino, *J. Colloid Interface Sci.*, 1978, **66**, 440-446.
41   T. Villalón, S. Su and U. Pal, Cham, 2016.
42   Y. Sato, T. Ejima, M. Fukasawa and K. Abe, *J. Phys. Chem.* 1990, **94**, 1991-1996.
43   M. V. Smirnov and V. P. Stepanov, *Electrochim. Acta*, 1982, **27**, 1551-1563.
44   A. R. Harikrishnan, P. Dhar, P. K. Agnihotri, S. Gedupudi and S. K. Das, *The European Physical Journal E*, 2017, **40**, 53.
45   G. Wang, H. Zhang, H. Wang, Q. Zhu, C. Li and H. Shan, *J. Catal.*, 2016, **344**, 606-608.
46   O. A. Bariås, A. Holmen and E. A. Blekkan, *J. Catal.*, 1996, **158**, 1-12.
47   S. E. Lohse, N. D. Burrows, L. Scarabelli, L. M. Liz-Marzán, and C. J. Murphy, *Chem. Mater.*, 2014, **26**, 34-43.
48   C.-K. Tsung, J. N. Kuhn, W. Huang, C. Aliaga, L.-I. Hung, G. A. Somorjai and P. Yang, *J. Am. Chem. Soc.*, 2009, **131**, 5816-5822.
49   M. R. Langille, M. L. Personick, J. Zhang and C. A. Mirkin, *J. Am. Chem. Soc.*, 2012, **134**, 14542-14554.

Table of contents (TOC)